ELSEVIER

Biophysical Chemistry 91 (2001) 49–60

Biophysical Chemistry

www.elsevier.nl/locate/bpc

# Theoretical analysis of the molecular determinants responsible for the $K^+$ channel blocking by aminopyridines

A. Niño*, C. Muñoz-Caro

*Grupo de Química Computacional, E. S. Informática. Universidad de Castilla-La Mancha, Paseo de la Universidad 4, 13071 Ciudad Real, Spain*

Received 21 December 2000; received in revised form 5 March 2001; accepted 7 March 2001

**Abstract**

This work presents a theoretical analysis of the molecular determinants responsible for the pharmacological activity ($K^+$ channel blocking) of aminopyridines. Thus, DFT theory at the B3LYP/cc-pVDZ level is applied to a series of active compounds: 2-aminopyridine, 3-aminopyridine, 4-aminopyridine, 3,4-diaminopyridine, and 4-aminoquinoleine. The two forms present in the biological environment, neutral and cationic (protonated), are considered in vacuum as well as in aqueous solution. The results show pyramidal and planar structures for the neutral and cationic forms, respectively. An analysis of the topology of the electron density show that an increase in conjugation between the pyridine ring and the amine group is responsible for the observed planarity of the protonated forms. By computing the Laplacian of the charge density we found the pyridine nitrogen to be the preferred protonation site, as a consequence of a much higher curvature of the charge density field. Also, from three-dimensional (3D) isoLaplacian diagrams a common reactivity pattern is only found in the charged forms. This reactivity pattern implies that interaction with the biological receptor site is mediated by electrostatic interactions and hydrogen bonding. Development of a physical–mathematical model allows identification of the specific relationship of the pharmacological activity index with the affinity for the receptor and the protonation ability. 

*Keywords:* $K^+$ channel blocking; Theoretical modelling; Aminopyridines

* Corresponding author. Tel.: +34-926295362; fax: +34-926295354.
*E-mail address:* quimcom@uclm.es (A. Niño).

0301-4622/01/$ - see front matter 
PII: S0301-4622(01)00151-X

## 1. Introduction

Aminopyridines are bioactive *N*-heterocyclic tertiary amines that increase the strength of the nerve signal [1]. These compounds exert their action by inhibiting the voltage-dependent $K^+$ channels [2] and hence maintain the presynaptic action potential. In this form the calcium influx is enhanced, leading to an increase in the release of neurotransmitter [3]. Due to their ability to facilitate nerve transmission, aminopyridines have been applied to reverse anaesthesia and muscle relaxation [4]. In addition, they have been proposed as drugs for the treatment of multiple sclerosis [5], myasthenia gravis [6], spinal cord injuries [7], botulism [8] and Alzheimer's disease [9].

Aminopyridines are weak bases, $pK_a \approx 9.0$, and thus they can exist in neutral or cationic (protonated) form at physiological pH. This characteristic complicates the elucidation of the way and site of action. Initial studies on 4-aminopyridine (4-AP) [10,11] show that this compound blocks the potassium channel when applied internally or externally to squid axons. Experimental studies [12,13] show that when 4-AP was externally applied, an increase of the external pH enhances the depth of block and the rate of onset. Since the basic medium would favour the neutral, lipid-soluble species, these results suggested an internal site of action. Studies by Kirsch and Narahashi [14] found that the blocking strength is maintained as long as the cationic form concentration is maintained constant in the intracellular medium. Similar results were obtained by Molgó et al. [3] analysing the effect of the variation of the external pH. All these facts show an intracellular active site with the cationic form as the active species. More recent experimental studies [15,16] also arrive at the same conclusions. At present, the specific nature of the receptor site is still unknown. However, the reversal of the action of aminopyridines when washing the nervous cells with solutions of decreasing pH values [3] show that the interaction with the intracellular receptor is essentially reversible (non-covalent).

The first theoretical study of aminopyridines from a pharmacological point of view was carried out by Peradejordi et al. [17]. Using partially optimised geometries and the virtual charge (solvaton) model [18] for solvation, these authors performed a semiempirical CNDO/2 study of the molecular electrostatic potential (MEP) on a series of active compounds. A common reactivity pattern was only found for the cationic species, in agreement with the experimental findings. Despite the interest of its applications, just a few theoretical studies on aminopyridines have been performed. MNDO calculations have been done on 2AP [19], whereas 2AP and 3AP dimers have been considered at the B3LYP/6-31G(d, p) level [20]. At present, the most complete work is a general structural study within a series of amine compounds including 2-AP, 3-AP and 4-AP [21].

Theoretical studies are of interest for the rationale of the action mechanism of bioactive compounds. In particular, the MEP can be useful to determine the sites for electrophilic attack [22,23]. However, identification of reactivity patterns based on the MEP exhibits an intrinsic drawback, since the MEP is obtained through the classical electrostatic potential [24]. Thus, it is not possible to determine sites for nucleophilic attack because the zones of positive potential are not necessarily expressing affinity for nucleophiles but, rather, the concentrated nature of the nuclear charges [25]. A more general and rigorous approach is based in Bader's Atoms In Molecules (AIM) theory [24,26,27]. AIM theory relies on the electron density, $\rho$, to reformulate chemical concepts such as atoms, bonds, electron pairs or reactivity. As well as the MEP, the electron density is a physically observable magnitude, independent of any arbitrary partition of the molecular orbital space [28]. This approach is in touch with the spirit of the density functional theory, which establishes that the total electronic density is the fundamental magnitude in many-electron systems [29]. AIM theory permits, following the Lewis standpoint of a chemical reaction, to determine the electrophilic and nucleophilic zones of a molecule from the topology and topography of the Laplacian of the charge density, $\nabla^2\rho$ [24,26,27].

In this work we present a detailed theoretical study of the molecular determinants responsible for the biological activity of aminopyridines. The following series of compounds, for which in vitro

activity data do exist [3], are considered: 2-aminopyridine (2-AP), 3-aminopyridine (3-AP), 4-aminopyridine (4-AP), 3,4-diaminopyridine (3,4-DiAP), and 4-aminoquinoleine (4-AQ). To use a realistic description for each molecule, we determine fully optimised geometries, at a correlated level, both in vacuum and in aqueous solution. The molecular basis for the pyridine nitrogen being the preferred protonation site, and its dependence with the solvent, is determined and analysed. The common reactivity pattern needed for the biological response is also investigated by means of three-dimensional (3D) diagrams of $\nabla^2\rho$. Finally, a physical–mathematical model is built to explain and model the observed variation of activity to the light of the computed reactivity data.

## 2. Theoretical methods

Molecular structures, and Atoms In Molecules properties are obtained at the correlated level applying density functional theory (DFT) by means of the B3LYP method. The hybrid B3LYP method is used since it is found to lead to reliable structures and harmonic vibrational frequencies for equilibrium structures [30–32]. With B3LYP we have used the correlation consistent, double-zeta, cc-pVDZ basis set [33], which includes by definition polarisation functions on hydrogen and heavy atoms.

To have a realistic description of the molecular behaviour in aqueous solution (dielectric constant, $\varepsilon = 78.39$) the solvent effect is considered by means of the Polarisable Continuum Model (PCM) [34,35]. In this method, a van der Waals surface type cavity is used as well as a detailed description of the electrostatic potential, and an appropriate parameterisation for the cavity/dispersion contribution based on the surface area. The PCM model maintains the expense of computational resources within reasonable limits applying, however, a realistic description of the molecular shape. Both in vacuum and solution, the molecular geometries considered are fully optimised. The calculations are carried out using the GAUSSIAN 98 package [36].

Atoms in Molecules theory is applied from the DFT one-electron density, ρ, by means of the MORPHY98 package [37].

## 3. Results and discussion

### 3.1. Molecular structures

Fig. 1 shows the structure and numbering convention of neutral aminopyridines. The protonated species contain an additional hydrogen at the N1 site. The most interesting structural feature relates to the amine group conformation. The planar or pyramidal structure of the amine group is of importance from a biophysical standpoint, since it can be related to the DNA structure and to molecular recognition processes [38,39]. Table 1 collects the structural data for the amine group in our series of aminopyridines, using the notation defined in Fig. 2. Our data are compared to the available MP2/6-311G(2df,p) data in vacuum for 2-AP, 3-AP and 4-AP [21].

Considering the C–N bond length, Table 1 shows that our results in vacuum are in good agreement with those of Bludský et al. [21]. The maximum difference found in the available data is $3 \times 10^{-3}$ Å. With respect to the dihedral angles the agreement is also good, maximum difference 3°, although the smaller force constant for dihedrals is translated into larger differences than for bond lengths. These data show that our structural results at the B3LYP/cc-pVDZ level are compa-

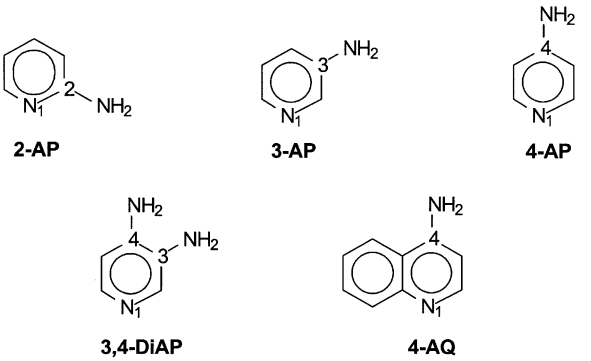


Fig. 1. Numbering convention and structure of neutral aminopyridines.

Table 1
Structural data in vacuum for the amine group in neutral and protonated aminopyridines (distances in Angstroms and angles in degrees)

| | $H_2NCC$ | $H_1NCX$ | NCCC | NCXX | NC |
|---|---|---|---|---|---|
| 2-AP[a] | −29.5 | 18.2 | −177.0 | 177.1 | 1.39 |
| 2-AP[b] | −32.5 | 18.7 | −177.0 | 176.8 | 1.39 |
| 3-AP[a] | −28.2 | 27.4 | −177.0 | 176.8 | 1.39 |
| 3-AP[b] | 25.1 | −29.5 | −177.0 | 176.6 | 1.39 |
| 4AP[c] | −23.0 | 23.3 | −177.0 | 177.0 | 1.38 |
| 3,4-DiAP[a,d] | 55.9 | −5.8 | 178.6 | −177.0 | 1.41 |
| 3,4-DiAP[a,e] | −18.4 | 36.3 | −179.0 | 179.3 | 1.39 |
| 4-AQ[a] | −32.6 | 16.8 | −179.0 | 178.3 | 1.39 |
| 2-APH + | 0.0 | 0.0 | 180.0 | 180.0 | 1.34 |
| 3-APH + | −0.1 | 0.1 | 180.0 | 180.0 | 1.35 |
| 4-APH + | −0.1 | 0.0 | 179.9 | 180.0 | 1.34 |
| 3,4-DiAPH +[d] | 55.0 | −0.2 | 179.6 | −177 | 1.39 |
| 3,4-DiAPH +[e] | −6.2 | 19.4 | 177.5 | −178 | 1.35 |
| 4-AQH + | 0.0 | 0.0 | 180.0 | 180.0 | 1.34 |

[a] This work, data obtained at the B3LYP/cc-pVDZ level.
[b] Data from [19] obtained at the MP2/6-311G(2df,p) level.
[c] This work. Büyükmurat et al. [19] only provides the planar structure corresponding to the first order saddle point for the amine group inversion.
[d] Amine group closest to the nitrogen in the pyridine ring, position 3.
[e] Amine group farthest to the nitrogen in the pyridine ring, position 4.

rable to the much higher (and computationally more expensive) MP2/6-311G(2df,p) level, in agreement with previous results [32]. The good equilibrium results provided by B3LYP can be associated to the way this exchange-correlation functional was developed. The values for the three empirical parameters defining the functional were obtained by Becke fitting to the atomisation energies, ionisation potentials, proton affinities and first-row atomic energies in the G1 molecule set [40]. Since the G1 molecular data are obtained at equilibrium [41], it can be expected the B3LYP functional to reproduce proper equilibrium properties.

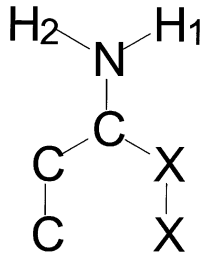


Fig. 2. Symbolic nomenclature for the amine group. $H_1$ is the hydrogen closest to the pyridine nitrogen. X means carbon (C) or nitrogen (N), depending on the molecule considered.

With respect to protonation in vacuum, Table 1 shows that in all the cases the amine group becomes coplanar with the aromatic ring. In addition, a clear shortening of the C–N bond occurs. Table 2 shows that a shortening is also observed upon protonation in aqueous solution. In contrast with the results in vacuum, the pyramidalisation of the amine group is reduced upon protonation without reaching a fully planar structure. On the other hand, comparison of Table 1 (vacuum), and Table 2 (solution) shows that in solution the amine group adopts a more symmetric structure. This behaviour can be explained as a consequence of the screening from the molecular environment produced by a dielectric medium of high dielectric constant.

The flattening of the amine group on protonation can be attributed to an increase of conjugation between the amine group and the aromatic ring. The situation can be clarified by applying the Atoms In Molecules theory (AIM). The AIM

Table 2
Structural data in aqueous solution, obtained at the B3LYP/cc-pVDZ level, for the amine group in neutral and protonated aminopyridines (distances in Angstroms and angles in degrees)

| | $H_2NCC$ | $H_1NCX$ | NCCC | NCXX | NC |
|---|---|---|---|---|---|
| 2-AP | −26.5 | 21.6 | −178.0 | 177.6 | 1.379 |
| 3-AP | −26.7 | 24.4 | −177.0 | 177.3 | 1.386 |
| 4-AP | −19.8 | 19.8 | −177.0 | 177.2 | 1.370 |
| 3,4-DiAP[a] | 45.8 | −13.0 | 178.4 | −177.3 | 1.402 |
| 3,4-DiAP[b] | −16.7 | 34.3 | −178.5 | 179.0 | 1.384 |
| 4-AQ | −24.0 | 15.3 | −179.0 | 179.0 | 1.370 |
| 2-APH + | −2.6 | 2.6 | −179.6 | 179.4 | 1.333 |
| 3-APH + | −15.8 | 15.6 | −177.8 | 177.9 | 1.357 |
| 4-APH + | −0.2 | 0.2 | −179.4 | 179.3 | 1.336 |
| 3,4-DiAPH + [a] | 43.5 | −11.9 | 176.9 | −175.7 | 1.386 |
| 3,4-DiAPH + [b] | 5.7 | −4.4 | 178.1 | −178.6 | 1.342 |
| 4-AQH + | −1.6 | 1.9 | −178.7 | 178.6 | 1.334 |

[a]Amine group closest to the nitrogen in the pyridine ring, position 3.
[b]Amine group farthest to the nitrogen in the pyridine ring, position 4.

characterises a bond by an atomic interaction line (AIL) [24,26,27] that is a line through the electron density, ρ, along which ρ is a maximum with respect to any neighbouring line. On the AIL lies the bond critical point (BCP), a second order saddle point where ρ reaches a minimum [24,26,27]. The value of the electronic density at the BCP for a given bond, $\rho_{b,}$ can be correlated to the concept of bond order [24,26,27,42], with higher values of $\rho_b$ corresponding to higher degrees of conjugation.

Table 3 collects the value of $\rho_b$ for the N–C bond in aminopyridines. In vacuum as well as in solution, we observe a clear increase in $\rho_b$ upon protonation, corresponding to an increase of conjugation with the pyridine ring.

In vacuum as well as in solution, the amine groups of 3,4-DiAP exhibit a clear distortion from the structures found for the other molecules. Both groups are rotated around the C–N bond with the amine group at position 3 (see Fig. 1), much more rotated than the second group. In these conditions we can expect an unfavourable position for conjugation. In vacuum as well as in solution this fact is observed in the value of the C–N bond length (see Tables 1 and 2), which is larger for the position 3 amine group than in any other molecule. The $\rho_b$ data (Table 3), also support this explanation. We can observe that $\rho_b$ for the position 3 amine group is always smaller than for position 4. The rotation of the amine groups can be attributed to steric hindrance between the two closest hydrogens of the $NH_2$ groups.

### 3.2. Protonation preference

AIM theory permits identification of protonation sites by means of the Laplacian of the charge density, $\nabla^2\rho$. AIM defines the valence-shell charge

Table 3
Value of the electronic density (in atomic units) at the BCP, $\rho_b$, for the pyridine ring-amine group bond in vacuum and in aqueous solution (data were determined from the one-electron density, ρ, calculated at the B3LYP/cc-pVDZ level)

| | Atom[a] | Vacuum | | Solution | |
|---|---|---|---|---|---|
| | | $\rho_b$[b] | $\rho_b$[c] | $\rho_b$[b] | $\rho_b$[c] |
| 2-AP | 2 | 0.309 | 0.334 | 0.312 | 0.34 |
| 3-AP | 3 | 0.300 | 0.325 | 0.305 | 0.324 |
| 3,4-DiAP | 3 | 0.290 | 0.306 | 0.295 | 0.309 |
| 3,4-DiAP | 4 | 0.301 | 0.328 | 0.305 | 0.328 |
| 4-AP | 4 | 0.305 | 0.332 | 0.312 | 0.334 |
| 4-AQ | 4 | 0.305 | 0.331 | 0.313 | 0.333 |

[a]Atom on the pyridine ring to which the amine group is bonded.
[b]Neutral forms.
[c]Protonated forms.

Table 4
Values of Laplacian of the charge density, $\nabla^2\rho$, in atomic units, at the Non-Bonded Critical Points (NBCP) of the nitrogen atoms in neutral aminopyridines (data in vacuum determined from the one-electron density, ρ, calculated at the B3LYP/cc-pVDZ level)

| | 2-AP | 3-AP | 3,4-DiAP | 4-AP | 4-AQ |
|---|---|---|---|---|---|
| N[a] | −3.52 | −3.76 | −3.65 | −3.63 | −3.57 |
| N[b,c] | −3.09 | −3.23 | −3.32 | −3.11 | −3.09 |
| N[b,d] | −1.77 | −1.71 | −3.16 | −1.80 | −1.73 |

[a] Pyridine nitrogen.
[b] Amine nitrogen.
[c] In 3,4-DiAP, NBCP placed in the apex of the pyramidal amine nitrogen at position 3, see text.
[d] In 3,4-DiAP, NBCP placed in the base of the pyramidal amine nitrogen at position 4, see text.

concentration (VSCC) as the outer molecular zone where $\nabla^2\rho < 0$. This zone is the one which, upon chemical combination, is distorted to yield non-bonded critical points (NBCP), which are minima in $\nabla^2\rho$ (maxima of charge concentration), corresponding in number and position to the electron pairs defined by the Lewis and related models [24,26,27]. NBCP correspond to nucleophilic zones where a protonation can occur.

NBCP have been determined for the pyridine and amine nitrogens. The results for the neutral molecules in vacuum and in solution are collected in Tables 4 and 5, respectively. As illustrated for 2-AP in Fig. 3a, we found in vacuum as well as in solution a single NBCP at the pyridine nitrogen. This NBCP is coplanar with the aromatic ring. On the other hand, as shown for 2-AP in Fig. 3b, two NBCP are found in all cases for the amine nitrogen, except for 3,4-DiAP. The first of these NBCP is placed at the apex of the pyramidic nitrogen (the place where the lone electron pair is usually represented). The second NBCP appears pointing to the base of the pyramid. In all cases the value of $\nabla^2\rho$ for the first NBCP is larger than for the second. The existence of these two NBCP can be explained to the light of the conjugation between the amine group and the aromatic ring. In absence of conjugation we can expect a single local maximum of charge concentration, i.e. an NBCP, corresponding to the lone electron pair placed in a hybrid orbital pointing to the apex of the pyramid. However, when the amine group is conjugated with the aromatic ring, we have the electron pair in something more similar to a two lobed $p_z$ orbital than to a hybrid orbital with a single lobe. Since we have not a pure $p_z$ orbital, the two lobes are not equivalent. In fact, the upper lobe should have a higher charge concentration, in agreement with the data collected in Tables 4 and 5.

On the other hand, 3,4-DiAP in vacuum (see Table 4), exhibits in the two amine groups, a single NBCP pointing to the apex of the pyramid. This is what can be expected from the previously shown low degree of conjugation for these amine groups. In solution, however, we have found that conjugation increases. In this case, two NBCP appear on each amine group (see Table 5), as in all other aminopyridines.

When we compare the value of $\nabla^2\rho$ at the different non-bonded critical points of the neutral species, we found a constant relationship. In all the molecules, in vacuum as well as in solution, the NBCP at the pyridine nitrogen exhibits the highest concentration of charge (see Tables 4 and 5). In terms of $\nabla^2\rho$ the difference is approximately 0.5 a.u. in absolute terms. Since we do not have a relation between $\nabla^2\rho$ and $\Delta G$, we cannot deduce that the pyridine nitrogen is the only

Table 5
Values of Laplacian of the charge density, $\nabla^2\rho$, in atomic units, at the Non-Bonded Critical Points (NBCP) of the nitrogen atoms in neutral aminopyridines (data in aqueous solution determined from the one-electron density, ρ, calculated at the B3LYP/cc-pVDZ level)

| | 2-AP | 3-AP | 3,4-DiAP | 4-AP | 4-AQ |
|---|---|---|---|---|---|
| N[a] | −3.45 | −3.67 | −3.53 | −3.50 | −3.45 |
| N[b,c] | −2.95 | −3.09 | −3.19 | −2.88 | −2.83 |
| N[b,d] | −1.70 | −1.68 | −1.54 | −1.83 | −1.81 |
| N[e,c] | – | – | −3.02 | – | – |
| N[e,d] | – | – | −1.64 | – | – |

[a] Pyridine nitrogen.
[b] Amine nitrogen. In 3,4-DiAP corresponds to position 3.
[c] NBCP placed in the apex of the pyramidal amine nitrogen, see text.
[d] NBCP placed in the base of the pyramidal amine nitrogen, see text.
[e] Amine nitrogen placed at position 4 in 3,4-DiAP.

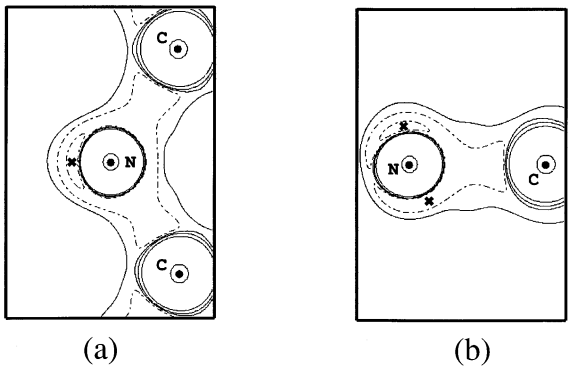


Fig. 3. Diagrams of isoLaplacian curves showing the location of the NBCP at the nitrogen atoms in 2-AP. The outer solid line corresponds to $\nabla^2\rho = 0$ a.u. (reactive surface), the two dashed lines correspond to values of $\nabla^2\rho = -0.5$ and $-3.0$ a.u. The solid circles represent the atomic nuclei and crosses the location of maxima of charge concentration. Case (a): pyridine nitrogen in the ring plane; case (b): amine nitrogen in a plane containing the C–N bond and perpendicular to the ring plane.

protonation site. However, the higher negative value of $\nabla^2\rho$, i.e. the higher curvature in this zone, implies that an approaching proton is directed (falls) to this zone rather than to the amine nitrogens. As in the case of formamide [26] the centre with the highest $\nabla^2\rho$ value seems to correspond to the preferred protonation site. In addition, Tables 4 and 5 show that in vacuum the absolute $\nabla^2\rho$ value at the NBCP of the pyridine nitrogen is slightly higher than the corresponding values in solution. Considering that to the light of several studies on series of amines [43] and phosphines [44] $\nabla^2\rho$ can be considered as an indicator of its proton affinity, we can expect the basicity of aminopyridines to be higher in the gas phase than in solution.

### 3.3. Common reactivity pattern

The reactive behaviour of a molecule can be determined from the spatial distribution of the Laplacian of the charge density. Negative zones of $\nabla^2\rho$ represent zones of locally concentrated charge density, and positive values of $\nabla^2\rho$ correspond to zones of locally depleted charge density. In particular, zones of minimal $\nabla^2\rho$ (as the NBCP) are candidates for an electrophilic attack, whereas zones of high positive value can be suitable for a nucleophilic agent [24,26,27].

To characterise the reactivity of a molecule we can use the $\nabla^2\rho = 0$ isosurface. This, so called, reaction surface surrounds all the bonded and non-bonded critical points on the Laplacian, i.e. the nucleophilic sites, being the outer limit of the valence shell concentration charge (VSCC). On the reactive surface the zones of charge depletion appear as holes around a nucleus, and nucleophiles are oriented to these holes [24,26,27]. Together with the NBCP, the reactive surface provides a 3D schema of the expected reactivity of a molecular system. In this work we introduce the use of another isosurface of $\nabla^2\rho > 0$, which permits us to visualise the location of nucleophilic zones (in our case the electron pairs of nitrogen). On this new surface the nucleophilic zones are exposed, i.e. they appear as holes.

Applying the following line of reasoning to a series of bioactive compounds, we can establish that a common reactivity pattern needs a common reactive surface as a prerequisite. To analyse the behaviour of aminopyridines in the physiological medium we have computed the reactive surface for the neutral and protonated forms in solution, complemented with a $\nabla^2\rho = 0.2$ a.u. surface (see Figs. 4 and 5). These figures reveal no holes exposing nuclei in the reactive surface. Thus, our molecules are not appropriate for an approaching nucleophile.

From an electrophilic point of view, we observe in the neutral forms (Fig. 4), that the reactive surfaces are not superimposible. This fact is a consequence of the existence of the NBCP on the pyridine nitrogen, which changes its position relative to the amine group from molecule-to-molecule. On the other hand, in the protonated species (Fig. 5), we found that the reactive surfaces are clearly equivalent along the series of compounds, since now there is no NBCP on the pyridine nitrogen. Compared with the $\nabla^2\rho = 0.2$ a.u. surface we observe, in the neutral compounds, two holes corresponding to the electron pairs on the pyridine and amine nitrogens (see Fig. 4). The relative positions of these holes vary from molecule-to-molecule. However, for the proto-

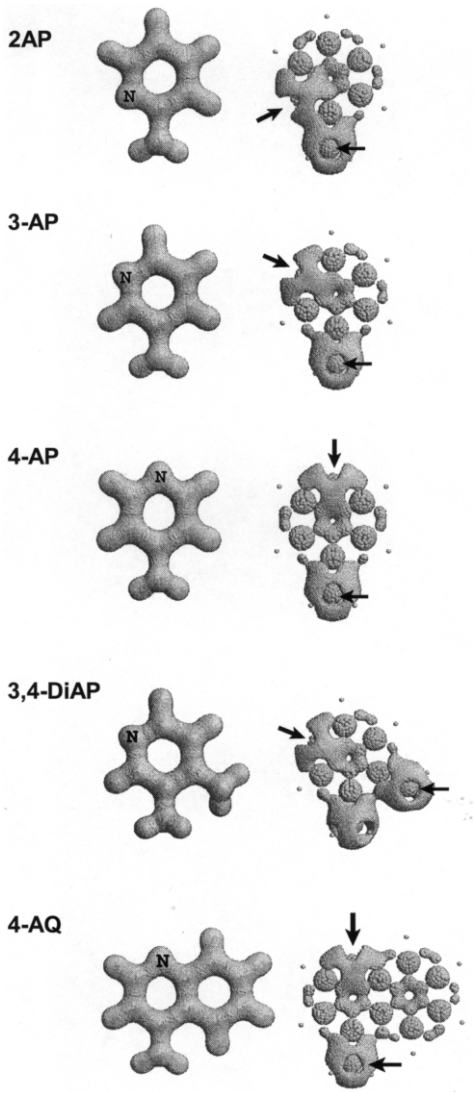


Fig. 4. 3D representation of surfaces of constant $\nabla^2\rho$ value for the series of neutral aminopyridines in aqueous solution. For each molecule the left case corresponds to the reactive surface ($\nabla^2\rho = 0$ surface), whereas the right case shows the $\nabla^2\rho = 0.2$ a.u. surface. The isosurfaces are represented as a superposition of small spheres. As a reference, the pyridine nitrogen is labelled in the $\nabla^2\rho = 0$ surface. In the $\nabla^2\rho = 0.2$ a.u. surface the spheres around the nitrogen and carbon atom correspond to the K atomic shell. The black arrows point to the electron pairs location. In 3,4-DiAP the second amine group exhibits another hole (electron pair) not visible in the draw.

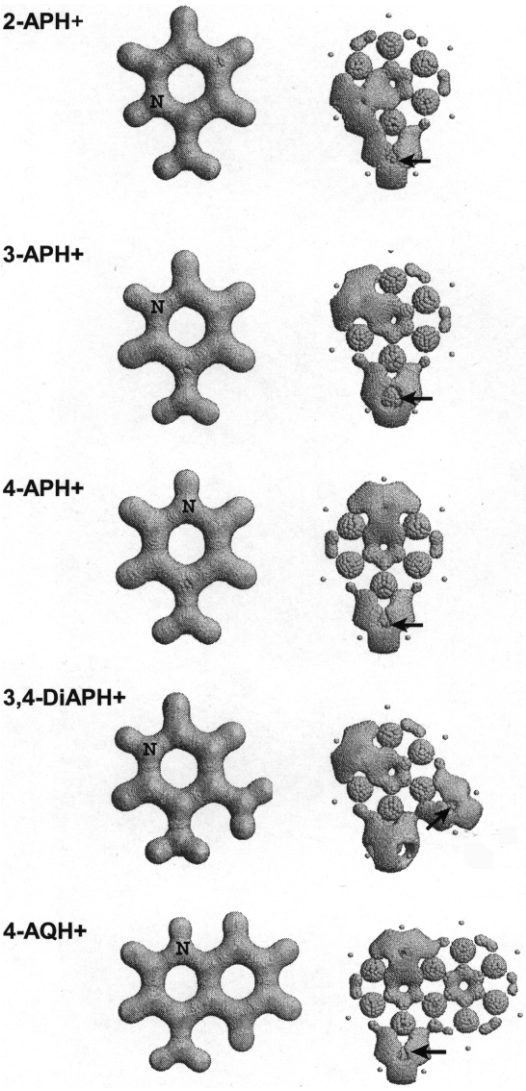


Fig. 5. 3D representation of surfaces of constant $\nabla^2\rho$ value for the series of protonated aminopyridines in aqueous solution. For each molecule the left case corresponds to the reactive surface ($\nabla^2\rho = 0$ surface), whereas the right case shows the $\nabla^2\rho = 0.2$ a.u. surface. The isosurfaces are represented as a superposition of small spheres. As a reference, the pyridine nitrogen is labelled in the $\nabla^2\rho = 0$ surface. In the $\nabla^2\rho = 0.2$ a.u. surface the spheres around the nitrogen and carbon atom correspond to the K atomic shell. The black arrows point to the electron pair location. In 3,4-DiAPH$^+$ the second amine group exhibits another hole (electron pair) not visible in the draw.

nated forms (Fig. 5), only one hole appears on the amine nitrogen, being possible to superimpose the structures. Thus, the observed common reactivity behaviour of our series of compounds must be due solely to the charged species. The common reactivity pattern appears, on one hand, because of the loss of pyridine NBCP, i.e. the existence of a positive charge, and, on the other hand, by the existence of an NBCP on the amine nitrogen. These results are in agreement with the CNDO/2, 2D study of the electrostatic potential of Peradejordi et al. [17].

In light of the present results, and as previously proposed [17], the pharmacophore should involve the positive charge and the nucleophilic nature of the electron pair on the amine group. Thus, the receptor site should bear a negatively charged residue and at least a group able to interact reversibly with the amine NBCP, i.e. able to form a hydrogen bond.

### 3.4. Modelling the activity

The biological activity of aminopyridines involves the protonation of the neutral species and the interaction with the receptor site at the $K^+$ channel. A formal model can be built starting from an amount of neutral compound placed in the intracellular medium. Assuming that the initial concentration of neutral aminopyridine is $C$ and given the protonation equilibrium:

$$APH^+ \rightleftarrows AP + H^+ \tag{1}$$

we have:

$$C = AP + APH^+ \tag{2}$$

Considering that the active form is the $APH^+$, and representing the concentration of active sites by $S$ we have for the equilibrium between the active site and the protonated aminopyridine:

$$K = (S \cdots APH^+)/(S \cdot APH^+) \tag{3}$$

where $S \cdot\cdot APH^+$ represents the concentration of the active site-protonated aminopyridine complex.

From the definition of an acidity constant for Eq. (1) and using Eq. (2), we obtain,

$$AP = K_a C/(H^+ + K_a) \tag{4}$$

Since the number of $APH^+$ molecules is higher than the number of active sites we can assume,

$$S = S \cdot\cdot APH^+ \tag{5}$$

Substitution of Eqs. (2), (4) and (5) into Eq. (3) yields,

$$K = (H^+ + K_a)/C \cdot H^+ \tag{6}$$

In turn, the $K$ constant is related to the Gibbs energy variation of the reaction by,

$$K = \exp[-\Delta G/RT] \tag{7}$$

where $\Delta G$ is, in pharmacological terms, the affinity for the receptor.

The experimental activity index for aminopyridines is the extracellular concentration of compounds producing, in vitro, the same biological response [3]. This magnitude is not the total concentration $C$, which is intracellular, but is directly related to it. Thus, we obtain $C$ from Eq. (6) after substitution of Eq. (7). Taking natural logarithms, we get:

$$\ln C = \Delta G/RT + \ln[(H^+ + K_a)/H^+] \tag{8}$$

Eq. (8) shows two factors determining the value of the activity index. The first one is the variation of Gibbs energy in the reaction, which depends on the variation of the translational, rotational and vibrational degrees of freedom. The second factor represents the influence of the concentration of the protonated form at a given pH. As seen in Eq. (8), this factor depends on the acidity constant, $K_a$. The higher this second factor, the smaller the concentration of the active (protonated) form. Eq. (8) with its two factors, explains the observation by Molgó et al. [3] that the relative activity does not have a direct relationship on the $pK_a$.

Eq. (8) can be useful to qualitatively interpret the experimental variation of activity to the light

of our computed reactivity data. Table 6 collects the $pK_a$ values and the activity at physiological pH (7.2) for the considered series of aminopyridines [3]. It also collects the values of $\nabla^2\rho$ at the NBCP on the amine nitrogen for the protonated forms in solution. We observe two zones corresponding to a difference in the logarithmic term of several orders of magnitude. The zone with the smaller value corresponds to the most active compounds (3,4-DiAP, 4-AP and 4-AQ). Within this zone the logarithmic term is almost constant and the activity follows the order, in absolute value, of $\nabla^2\rho$ at the minimum NBCP, i.e. the affinity for the receptor. In the second zone the logarithmic term is much greater and its variation corresponds inversely to the variation of activity. The variation of activity, however, follows once more the variation in absolute value of $\nabla^2\rho$ at the minimum NBCP. Then, for comparable values of the logarithmic term, the activity is determined by the affinity. This fact is what we can expect on statistical thermodynamics grounds. Different values of $\nabla^2\rho$ can be correlated, in the spirit of the DFT theory, to energetic changes. $\Delta G$ depends exponentially on the energy levels via the partition function. Thus, we can expect small energetic changes to be associated to higher variations of $\Delta G$. In addition, the relationship between $C$ and $G$ is also exponential. These two facts taken together explain that small variations in $\nabla^2\rho$ are reflected in large variations of total concentration, $C$, making the affinity term the leading one in Eq. (8).

## 4. Conclusions

In this work, we have performed a theoretical analysis of the reactive properties responsible for the biological activity of aminopyridines. The behaviour of a series of active molecules in neutral and protonated form is considered in vacuum and in aqueous solution. The study is carried out applying the Atoms In Molecules theory, from the B3LYP/cc-pVDZ one-electron density.

After full geometry optimisation we found a pyramidal/planar conformation for the amine group in the neutral/protonated forms. The same behaviour is found in vacuum and in solution. Analysis of the electron density values at the bond critical point in the pyridine ring–amine nitrogen bond shows an increase of conjugation in the protonated forms. This increase is responsible for the observed planarity.

The protonation sites are identified from the Non-Bonded-Critical-Points (NBCP) on the Laplacian of the charge density. The highest value of $\nabla^2\rho$ found on the NBCP at the pyridine nitrogen identifies it as the preferred protonation site. This fact is due to the high curvature of the electron density distribution in this zone.

An analysis of the reactive, $\nabla^2\rho = 0$, and the $\nabla^2\rho = 0.2$ a.u. isosurfaces is carried out in solution for the neutral and protonated forms of the considered series of aminopyridines. The results show that the protonated forms share a common reactivity pattern. Thus, the protonated molecules are identified as the active species. The activity is

Table 6
Laplacian of the charge density, $\nabla^2\rho$, and value of the ln $[(H^+ + K_a)/H^+]$ term for the considered series of protonated aminopyridines in solution [the table also collects the experimental $pK_a$ and activity values; calculations at physiological pH (7.2)]

| | $pK_a$[a] | ln $[(H^+ + K_a)/H^+]$ | Activity ($\mu$M)[b] | $\nabla^2\rho$[c] |
|---|---|---|---|---|
| 2-AP | 6.86 | 1.159 | 91.2 | −2.26/−2.13 |
| 3-AP | 5.98 | 2.868 | 38.2 | −2.74/−1.92 |
| 3,4-DiAP | 9.08 | 0.013 | 0.5 | −3.12//−2.31/−2.06 |
| 4-AP | 9.17 | 0.011 | 3.2 | −2.16/−2.14 |
| 4-AQ | 9.17 | 0.011 | 26.0 | −2.15/−2.07 |

[a] Molgo et al. [45].
[b] In vitro, effective dose of neutral compound that produces the same effect on the sciatic nerve of *Rana esculenta* [3].
[c] Value of $\nabla^2\rho$ at the two NCBP on the amine nitrogen. In 3,4-DiAP the first value corresponds to the amine nitrogen NBCP found at position 3. The next couple of values corresponds to the two NBCP on the amine nitrogen at position 4.

associated to the existence of a nucleophilic centre (the amine nitrogen) and a positive charge. The corresponding complementary receptor site should involve an anionic form and at least a group able to form a hydrogen bond.

A model accounting for the dissociation equilibrium of the aminopyridine, and the formation of the aminopyridine–receptor site complex is developed. The model permits a qualitative interpretation of the observed in vitro activity in terms of the Gibbs energy of the aminopyridine–receptor site interaction (affinity) and the acidic constant of the aminopyridine. The results show that for a given range of $pK_a$ values the affinity is the determining factor of activity.

## Acknowledgements

The authors thank the DGESIC (grant # PM98-0073) and the Universidad de Castilla-La Mancha for financial support.

## References

[1] J. Molgó, M. Lemeignan, F. Peradejordi, P. Lechat, Effects présynaptiques des aminopyridines a la junction neuromusculaire de vertébrés, J. Pharmacol. (Paris) 16 (Suppl. II) (1985) 109–144.

[2] G.E. Kirsch, T. Narahashi, 3,4-Diaminopyridine. A potent new potassium channel blocker, Biophys. J. 22 (1978) 507–512.

[3] J. Molgó, M. Lemeignan, P. Lechat, F. Peradejordi, Increase in evoked transmitter release from motor nerve terminals by some amino *N*-heterocyclic compounds. I, Eur. J. Med. Chem. 20 (1985) 149–153.

[4] C. Carlsson, I. Rosen, E. Nilsson, Can 4-aminopyridine be used to reverse anaesthesia and muscle relaxation? Acta Anaesthesiol. Scand. 27 (1993) 87–90.

[5] S.R. Schwid, M.D. Petrie, M.P. McDermott, D.S. Tierney, D.H. Maso, A.D. Goodman, Quantitative assessment of sustained-release 4-aminopyridine for symptomatic treatment of multiple sclerosis, Neurology 48 (1997) 817–821.

[6] K.M. McEvoy, A.J. WindebankN, J.R. Daube, P.A. Low, 3-4-Diaminopyridine in the treatment of Lambert–Eaton myasthenic syndrome, N. Engl. J. Med. 321 (1989) 1567–1571.

[7] J.L. Segal, S.R. Brunnemann, 4-Aminopyridine improves pulmonary function in quadriplegic humans with long-standing spinal cord injury, Pharmacotherapy 17 (1997) 415–423.

[8] L.C. Sellin, The action of botulinum toxin at the neuromuscular junction, Med. Biol. 59 (1981) 11–20.

[9] M. Davidson, J.H. Zemishlany, R.C. Mohs et al., 4-Aminopyridine in the treatment of Alzheimer's disease, Biol. Psychiatry 23 (1988) 485–490.

[10] H. Meves, Y. Pichon, Effects of 4-aminopyridine on the potassium current in internally perfused giant axons of the squid, J. Physiol. (Lond.) 251 (1979) 60P–62P.

[11] J.Z. Yeh, G.S. Oxford, C.H. Wu, T. Narahashi, Interactions of aminopyridines with potassium channels of squid axon membranes, Biophys. J. 16 (1976) 77–81.

[12] J.I. Gillespie, O.F. Hutter, The actions of 4-aminopyridine on the delayed potassium current in skeletal muscle fibres, J. Physiol. (Lond.) 252 (1975) 70P–71P.

[13] J. Molgó, H. Lundh, S. Thesleff, Potency of 3,4-diaminopyridine and 4-aminopyridine on mammalian neuromuscular transmission and the effect of pH changes, Eur. J. Pharmacol. 61 (1980) 25–34.

[14] G.E. Kirsch, T. Narahashi, Site of action and active form of aminopyridines in squid axon membranes, J. Pharmacol. Exp. Ther. 226 (1983) 174–179.

[15] J.R. Howe, J.M. Ritchie, On the active form of 4-aminopyridine: block of K + currents in rabbit Schwann cells, J. Physiol. 433 (1991) 183–205.

[16] D. Choquet, H. Korn, Mechanism of 4-aminopyridine action on voltage-gated potassium channels in lymphocytes, J. Gen. Physiol. 99 (1992) 217–240.

[17] F. Peradejordi, J. Molgó, M. Lemeignan, Increase in evoked transmitter release from motor nerve terminals by some amino *N*-heterocyclic compounds. II, Eur. J. Med. Chem. 20 (1985) 155–161.

[18] R. Constanciel, O. Tapia, On the theory of solvent effects. The virtual charge Model to represent the solvent polarization, Theor. Chim. Acta 48 (1978) 75–86.

[19] Y. Büyükmurat, E. Akalin, A.E. Özel, S. Akyüz, Calculation and analysis of IR spectrum of 2-aminopyridine, J. Mol. Struct. 482-483 (1999) 579–584.

[20] I. Król, M. Rospenk, L. Sobcyk, On the association of aminopyridines, J. Mol. Struct. 552 (2000) 213–221.

[21] O. Bludský, J. Šponer, J. Leszczynski, V. Špirko, P. Hobza, Amino groups in nucleic acid bases, aniline, aminopyridines, and aminotriazine are nonplanar: Results of correlated ab initio quantum chemical calculations and anharmonic analysis of the aniline inversion motion, J. Chem. Phys. 105 (1996) 11042–11050.

[22] E. Scrocco, J. Tomasi, Electronic molecular structure, reactivity and intermolecular forces: an heuristic interpretation by means of electrostatic molecular potentials, Adv. Quantum Chem. 11 (1978) 115–193.

[23] C. Muñoz-Caro, A. Niño, M.L. Senent, J.M. Leal, S. Ibeas, Modeling of protonation processes in acetohydroxamic acid, J. Org. Chem. 65 (2000) 405–410.

[24] R.F.W. Bader, A quantum theory of molecular structure and its applications, Chem. Rev. 91 (1991) 893–928.

[25] P. Politzer, S.J. Landry, T. Warnheim, Proposed procedure for using electrostatic potentials to predict an

interpret nucleophilic processes, J. Phys. Chem. 86 (1982) 4767–4771.
[26] R.F.W. Bader, Atoms In Molecules. A Quantum Theory, Oxford University Press, 1995.
[27] P. Popelier, Atoms In Molecules. An Introduction, Prentice Hall, 2000.
[28] A.D. Becke, K.E. Edgecombe, A simple measure of electron localization in atomic and molecular systems, J. Chem. Phys. 92 (1990) 5397–5403.
[29] F. Jensen, Introduction to Computational Chemistry. Chapter 6. Density Functional Theory, John Wiley & Sons, 1999.
[30] S.G. Stepanian, I.D. Reva, E.D. Radchenko, L. Adamowicz, Conformational behavior of α-alanine. Matrix-isolation infrared and theoretical DFT and ab initio study, J. Phys. Chem. A 102 (1998) 4623–4629.
[31] M. Lozynski, D. Rusinska-Roszak, H.-G. Mack, Hydrogen bonding and density functional calculations: The B3LYP approach as the shortest way to MP2 results, J. Phys. Chem. A 102 (1998) 2899–2903.
[32] A. Niño, C. Muñoz-Caro, M.L. Senent, Suitability of different levels of theory for modelling of hydroxamic acids, J. Mol. Struct. THEOCHEM 530 (3) (2000) 291–300.
[33] T.H. Dunning, Jr., Gaussian basis sets for use in correlated molecular calculations. I. The atoms boron through neon and hydrogen, J. Chem. Phys. 90 (2) (1989) 1007–1023.
[34] M. Cossi, V. Barone, R. Cammi, J. Tomasi, Ab initio study of solvated molecules: a new implementation of the polarizable continuum model, Chem. Phys. Lett. 255 (1996) 327–335.
[35] V. Barone, M. Cossi, J. Tomasi, A new definition of cavities for the computation of solvation free energies by the polarizable continuum model, J. Chem. Phys. 107 (1997) 3210–3221.
[36] M.J. Frisch, G.W. Trucks, H.B. Schlegel et al., Gaussian 98, Revision A.7, Gaussian, Inc., Pittsburgh PA, 1998.
[37] P.L.A. Popelier, MORPHY98, a topological analysis program with a contribution from R.G.A. Bone, UMIST, Manchester, England, EU (1998).
[38] J. Šponer, P. Hobza, Bifurcated hydrogen bonds in DNA crystal structures. An ab initio quantum chemical study, J. Am. Chem. Soc. 116 (1994) 709–714.
[39] J. Šponer, J. Florián, P. Hobza, J. Leszcynski, Nonplanar DNA base pairs, J. Biomol. Struct. Dyn. 13 (1996) 827–833.
[40] A.D. Becke, Density-functional thermochemistry. III. The role of exact exchange, J. Chem. Phys. 98 (1993) 5648–5652.
[41] J.A. Pople, M. Head-Gordon, D.J. Fox, K. Raghavachari, L.A. Curtiss, Gaussian-1 theory: a general procedure for prediction of molecular energies, J. Chem. Phys. 90 (1989) 5622–5629.
[42] R.F.W. Bader, T.S. Slee, D. Cremer, E. Kraka, Description of conjugation and hyperconjugation in terms of electron distributions, J. Am. Chem. Soc. 105 (1983) 5061–5068.
[43] T.-H Tang, W.-J Hu, D.-Y Yan, Y.-P. Cui, A charge density topological approach on the equilibrium gas-phase basicity of selected nitrogen-containing organic molecules, J. Mol. Struct. (THEOCHEM) 207 (1990) 327–331.
[44] S.T. Howard, J.A. Platts, Relationship between phosphine proton affinities and lone pair density properties, J. Phys. Chem. 99 (1995) 9027–9033.
[45] J. Molgó, M. Lemeignan, P. Lechat, Effects of 4-aminopyridine at the frog neuromuscular junction, J. Pharmacol. Exp. Ther. 203 (1977) 653–663.